RILEM Technical Letters (2026) 11: 8-17
https://doi.org/10.21809/rilemtechlett.2026.226

Nano silica admixtures: Salt ingress and reaction in mortar

Julien Hubert[1,*], Fengyin Du[1], Cibele De Araujo[1], O Burkan Isgor[1], W Jason Weiss[1]

[1]Oregon State University, USA

Received: 03 October 2025 / Accepted: 03 March 2026 / Published online: 30 March 2026

Abstract

This paper examines the influence of commercially available nano silica (NS) admixtures on salt ingress and reaction in mortar. A series of mortar mixtures at dosages ranging from 2.6 to 41.8 mL/kg were tested using isothermal calorimetry (IC), thermogravimetric analysis (TGA), low temperature differential scanning calorimetry (LTDSC), and chloride profiling. Thermodynamic modeling was used to support the experiments. IC showed that the heat of hydration was slightly higher (2-3%) than the reference mixture when the NS admixtures were used. TGA indicated up to 18% reduction in calcium hydroxide at low admixture concentrations (2.6 to 7.8 mL/kg), which is greater than the reduction that would be expected due to pozzolanic reactions alone. At higher admixture dosages (above the recommended dosages), the calcium hydroxide contents were similar to or higher than those of the reference mixture. LTDSC results showed up to a 30% reduction in calcium oxychloride (CaOXY) formation potential; however, this reduction may not be sufficient to avoid the potential damage associated with expansive CaOXY formation at concrete joints in pavements and flatwork. The NS admixtures did not affect chloride ingress profiles significantly. Thermodynamic calculations indicate that although the admixtures provide reactive silica that acts pozzolanically, the amount is relatively small compared to the admixture dosages used.

Keywords: Colloidal silica, Nano silica, Admixtures, Deicing salts, Hydration, Pozzolanic reaction.

1 Introduction

New admixtures are emerging in modern concrete. The goal of many of these admixtures is to improve the fresh and hardened properties of concrete. One family of admixtures that has recently emerged is those containing nano silica (NS) particles. ACI 241R-17 discusses recent developments in nanoscale additives highlighting how nanoparticles can enhance the densification of the microstructure of hardened cementitious systems through improved particle packing. Aggarwal et al. [1] describes how the high surface area to volume ratio of nanoparticles enables rapid reactions, but it can also cause particles to agglomerate if not properly dispersed.

NS can be considered as a supplementary cementitious material (SCM) in the size range of 1 to 1000 nm [2-5]. NS can be used in various forms but is often a slurry-type liquid additive where it can be blended with other materials to improve dispersion [6, 7]. Collepardi [8] discusses how ultra-fine amorphous NS reduces bleeding and segregation in self-consolidating concrete. Aggarwal et al. [1] reported that NS might improve compressive strength in mixtures containing only cement, while compressive strength may not improve in mixtures containing SCM. Sharaky et al. [9] reported that with NS additions of 1.5 and 3% by mass of cement, compressive strength increased and water absorption decreased.

NS has also been found to increase the rate of hydration, which has been attributed to NS acting as a nucleating agent and participating in pozzolanic reactions [10]. Hou et al. [11] investigated colloidal nano-silica at dosages primarily around 5 wt.% of cementitious materials, with additional data reported at lower dosages (0.5 and 1 wt.%). They showed that the calcium hydroxide (CH) production is similar or up to 2% greater when NS is used (due to nucleation and accelerated reaction); however, the CH reduces at later ages due to consumption by pozzolanic reactions. Belkowitz [12] compared plain pastes, pastes with silica fume, and pastes with NS of different particle sizes and showed that the CH content decreased with the addition of NS, presumably due to pozzolanic reactions. As the silica particle size increases (from the smallest nano silica to silica fume), the rate of the pozzolanic reaction decreased [3].

While the pozzolanic reaction is often mentioned for the benefits of concrete containing NS, at very early ages, from

*Corresponding author: Julien Hubert, E-mail: julien.hubert@oregonstate.edu

the time after mixing or right before initial set, there is a lack of CH present in the system (as shown in Figure 1). Gartner et al. [13] described how during the initial dissolution phase of hydration the calcium level is below CH saturation in the pore solution, and as such, one would not expect CH to precipitate until approximately the end of the induction period. This is consistent with data from Roy et al. [14], Diamond and Odler [15], and Sant et al. [16]. Yi and Feldman [17] reported that the addition of silica reduces both Ca^{2+} and OH^- ion concentration at early ages, hence promoting CH precipitation. Therefore, it appears that initially NS may serve as a nucleating agent, enabling a surface for C-S-H to form. Dissolved silica in the pore solution may also delay the precipitation of CH in favor of C-S-H formation, extending the induction period and delaying the acceleration period.

Tests performed using alternative forms of silica may help in understanding the role of NS on the performance of concrete [18]. For example, tetraethyl orthosilicate (TEOS) has often been used as a consolidant for hardened cementitious products and fired bricks [19]. TEOS use increases strength, reduces porosity, and decreases permeability by reacting with CH and lengthening the chains of C-S-H. Sandrolini et al. [20] confirmed that the use of TEOS resulted in pozzolanic reactions. Gaitero [21] used NMR to show that NS tetrahedra form, impacting the non-evaporable water. Yang et al. [22] reported when used in fresh cementitious mixtures, TEOS lengthened the induction period and reduced the calcium-to-silica ratio (Ca/Si) of the C-S-H.

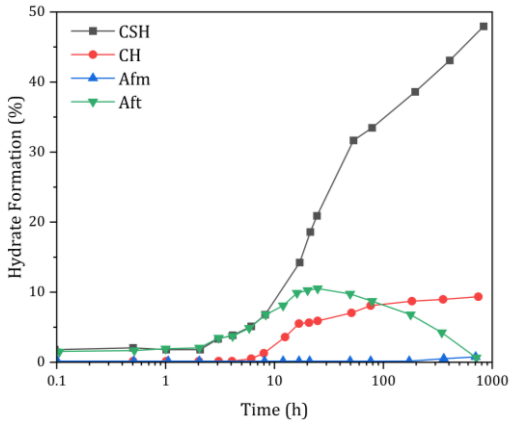

Figure 1. Formation of hydrates during the hydration kinetics of OPC (after [15]).

Yang et al. [22] showed that for low addition rates of TEOS (up to 1% by mass of cement) hydration was accelerated, while for higher dosages (3 and 5% by mass of cement) the opposite effect was observed. It was reported that the secondary tricalcium aluminate reaction peak shifted to earlier ages as the silica increased (occurring at nearly the peak hydration rate of the calcium silicates for 1% TEOS), resulting in a substantial reduction in the CSH reaction (which is similar to what is observed with an insufficient sulfate balance [23]).

In North America, NS has begun to be added to specifications. For example, the Indiana Department of Transportation (INDOT) permitted NS, noting the benefits of water retention, workability, pumpability, increased strength, and reduced permeability [24-26]. INDOT also permitted alternative curing, enabling NS to be used in place of water curing [27]. Similar interest in using NS exists in other parts of the world. As these materials become more widely used, it is important to understand their impact on the performance of cementitious systems.

NS are being pursued due to the expected benefits of water retention, workability, pumpability, increased strength, and reduced permeability. One question that arises is that most admixtures containing NS used in concrete typically contain relatively low NS dosages. As such, there are questions on whether, at these dosages, the full benefits generally associated with conventional SCMs can be achieved. The main objective of this paper is to provide answers to some of these questions. Specifically, this paper evaluates two NS admixtures at and above their recommended dosage levels to determine their impact on non-evaporable water, CH consumption, potential reaction with deicing salts to form CaOXY, and chloride ingress. This paper also aims to provide data that allows these materials to be compared to more conventional SCM sources.

2 Materials and methods

2.1 Materials

Commercially available, ASTM C595 [28] Type IL portland-limestone cement (PLC) with an interground limestone content of 11.73% was used for all the mixtures. The estimated Bogue composition of the PLC is 35% C_3S, 29% C_2S, 7% C_3A and 8% C_4AF (by mass). The chemical composition of the cement was determined using X-ray fluorescence from which the oxide composition was determined using the fused bead process. The fused beads were prepared by combining 1 g powder with 5 g flux. The flux composed of 49.75% lithium metaborate, 49.75% lithium tetraborate, and 0.50% lithium iodide was mixed gently in a platinum crucible and fused in a furnace for approximately 25 minutes at 1450°C. The chemical composition of the PLC used is provided in Table 1.

The sand used is graded standard sand that conforms to ASTM C778 [29]. It has a d50 of 0.375 mm. Tap water was used.

Table 1. Chemical composition of the Type IL portland-limestone cement (PLC).

Oxide (%)	Na_2O_{eq}	MgO	Al_2O_3	SiO_2	P_2O_5	SO_3	Cl
	0.14	3.38	4.33	19.28	0.04	3.62	0.01
	K_2O	CaO	TiO2	Mn_2O_3	Fe_2O_3	ZnO	LOI
	0.89	60.20	0.28	0.11	2.55	0.03	5.16

Two distinct types of NS admixtures have been considered in this study. Admixture A is an ASTM C494 [30] type S admixture designed to be used at dosage rates of 4 to 12 oz/cwt (2.6-7.8 mL/kg) cementitious material. The admixture contains non-crystalline silica and has a solid content of 31.8%. The product literature of this admixture reports that it can improve finishability, retain slump, increase viscosity,

enhance workability, and improve surface densification while retaining moisture to reduce evaporation rates in concrete [31]. Admixture B is an admixture designed to be used at dosage rates of 8 to 20 oz/cwt (5.2-13.1 mL/kg) cementitious material. The admixture is reported in product literature to be a NS designed to improve finishability, pumpability and workability. It is also reported to reduce evaporation and reduce evaporation from concrete [32]. Admixture B was measured to have a solid content of 32.4%.

Scanning Electron Microscopy (SEM) has been used on the dried solid fraction of the admixtures to estimate the nominal particle size. Based on the SEM observations, Admixture A exhibits an average particle size of approximately 48 nm, while Admixture B shows an average particle size of approximately 27 nm.

2.2 Pozzolanic Reactivity of Nano Silica

The pozzolanic reactivity of the NS has been evaluated using the Pozzolanic Reactivity Test (PRT) [33-35]. The sample is prepared by combining one-part pozzolan (in this case, the NS admixture rather than just the solid pozzolan), three parts CH and 0.5 M KOH solution. The paste is prepared following the procedure described in [36]. The test method combines CH consumption determined using thermogravimetric analysis (TGA) [33, 37] with the heat release measured for 240-hours (10-days) at a temperature of 50°C using an isothermal calorimeter. The extent of the pozzolanic reaction is determined by measuring the amount of CH consumed and heat generated by the pozzolanic reactions after ten days at 50°C. These values are superimposed on a plot with theoretical CH consumption and heat release lines for reference SiO_2 and Al_2O_3 systems at equilibrium at different theoretical maximum reactivities (Figure 2) [34, 38]. Depending on the relative position of the point represented by CH consumption and heat release with respect to the theoretical lines, the DOR* can be quantified. This test provides a methodology for measuring the amount of reactive versus non-reactive components of a pozzolan, which is quantified as the maximum degree of reactivity (DOR*). As shown in Figure 2, Admixture A was found to have a DOR* of 58%, and Admixture B was found to have a DOR* of 41%. These reactivities are higher than a large range of silicious pozzolanic materials (e.g., fly ash) [39]; therefore, they show promise to act pozzolanically.

2.3 Mixture proportions

Eleven different mixtures were considered in this study and are presented in Table 2. These mixtures present 45% sand by volume and a water-to-binder ratio (w/b) of 0.42. While the presence of sand may introduce local variability in paste content, this effect was minimized by grinding and homogenizing large sample masses prior to subsampling for all analyses. The first mixture is a plain mortar mixture (i.e., Reference). Mixtures A1 to A5 have been prepared with an increasing dosage of admixture A. Mixtures B1 to B5 have been similarly prepared with an increasing dosage of admixture B.

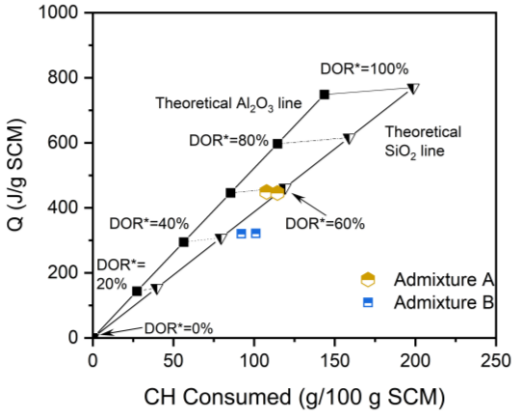

Figure 2. Pozzolanic reactivity (DOR*) of the studied admixtures measured using the PRT test (replicate testing shown).

Table 2. Mixture proportioning.

Material	Standard Graded Sand (kg/m³)	Type IL PLC (kg/m³)	Water (kg/m³)	Admixture		W/B (-)	L/S (-)
				oz/cwt	wt.% of cementitious		
Reference	1192.5	744.0	310.0	0.0	0	0.42	0.16
A1	1192.5	744.0	310.0	4	0.26	0.42	0.16
A2	1192.5	744.0	310.0	8	0.52	0.42	0.16
A3	1192.5	744.0	310.0	12	0.78	0.42	0.16
A4	1192.5	744.0	310.0	32	2.08	0.43	0.17
A5	1192.5	744.0	310.0	64	4.17	0.44	0.17
B1	1192.5	744.0	310.0	4	0.25	0.42	0.16
B2	1192.5	744.0	310.0	8	0.52	0.42	0.16
B3	1192.5	744.0	310.0	12	0.78	0.42	0.16
B4	1192.5	744.0	310.0	32	2.08	0.43	0.17
B5	1192.5	744.0	310.0	64	4.17	0.44	0.17

2.4 Mixing procedure

The commercial NS products used in this study are supplied as colloidal suspensions. The dispersant trisodium 1-(4-sulfonatophenyl)-4-(4-sulfonatophenyl azo)-5-pyrazolone-3-carboxylate (Tartrazine) present in the products contributes to particle dispersion. The colloidal solution also exhibits a high pH (9-11 for admixture A [40] 9-10 for admixture B [41]) which generates a negatively charged particle surface and helps limit aggregation. Therefore, no additional dispersion steps were required, and the admixture has been added directly to the batching water as suggested in the product technical sheet. Once the material was mixed, it was cast in 50.8 mm × 101.6 mm (2in × 4in) cylindrical molds in two lifts,

vibrating to provide compaction after each lift. The molds were then sealed with their lids, taped with duct tape and double-bagged using zip-lock bags to minimize moisture loss. The samples were stored at 23 ± 2°C for 91 days in sealed condition.

3 Methods

3.1 Degree of hydration (DOH, non-evaporable water content)

To measure the degree of hydration, 1 cm slices were cut into the cylindrical mortar samples, crushed, and then dried in an oven at 105°C for 24 h. Next, approximately 6g of the material was placed in ceramic crucibles, weighed, and then placed in a furnace at 1050°C for 3 h. The weights were recorded to monitor the evaporable and non-evaporable water contents. The measurements were corrected to account for the loss on ignition (LOI) of the constituent materials.

3.2 Thermogravimetric analysis (TGA)

Thermogravimetric analysis (TGA) was performed to assess the CH and $CaCO_3$ contents of the samples. A 1 cm slice was cut from the cylindrical mortar samples and pulverized into a fine powder passing through a 75-µm mesh size (No. 200) sieve. After the powder was ground, it was stored in an oven set at 105 ± 2°C for 24 h to remove excess water. 30–40 mg of the powder was placed into a platinum pan and loaded into the TGA instrument, and heated at a rate of 10°C/min under a nitrogen purge up to 1000°C. The mass loss was recorded during the experiment to quantify CH using the weight loss between 350°C and 550°C, and calcium carbonate ($CaCO_3$) using the weight loss between 500°C to 700°C [42]. Two replicates of TGA per mixture were considered for this study.

3.3 Low Temperature Differential Scanning Calorimetry (LTDSC)

Low temperature Differential Scanning calorimetry (LT-DSC) was performed to measure the amount of CaOXY formed due to the reaction of cement paste in contact with de-icing salts [43, 44]. A 1 cm slice was cut from the cylindrical mortar samples and pulverized into a fine powder passing through a 75-µm mesh size (No. 200) sieve. Grinding was conducted immediately prior to testing. Pulverization exposes fresh surfaces, which may promote limited additional hydration; therefore, subsequent handling time was minimized.

10 ± 0.5 mg of powder was mixed with an equal mass of a solution of calcium chloride (20% $CaCl_2$ by mass) in a high volume DSC pan. The powder to solution mass ratio resulting from this procedure is 1 which lead to a CH to $CaCl_2$ molar ratio lower than 3, ensuring the complete consumption of the CH and the formation of the maximum possible amount of CaOXY [44, 45]. The time between mixing and testing was kept below 1 hour to limit additional hydration reactions. However, small variations in handling time may influence the extent of early reactions from one sample to another. The samples were initially held at 25°C for at least 50 minutes but less than 1 hour, allowing any initial heat release associated with the hydration of exposed unreacted surfaces of the cementitious materials to occur. Then, the temperature is reduced to –90°C at a rate of 3°C/min. A low-temperature loop is run from –90 to –70 to –90°C at a rate of 3°C/min. Finally, the temperature is increased to 50°C at a rate of 0.25°C/min. The minimum temperature and the low temperature loop are applied to ensure freezing of the eutectic solution, which occurs at approximately –54°C. The maximum temperature is similarly chosen to ensure the phase transition of CaOXY, which occurs between 30 and 40°C [45] for the salt concentration used. The latent heat associated with the melting can be measured between the two temperature steps of the transition, and by comparing the latent heat with that measured for pure CaOXY (186 J/g) [44] the amount of CaOXY formed in any chosen mixture can be quantified.

As discussed in [44, 45], this LT-DSC protocol provides an upper-bound estimate of CaOXY formation potential due to the imposed CH-to-$CaCl_2$ ratio and saturation conditions. Accordingly, the results are interpreted comparatively between mixtures rather than as absolute values of in-situ CaOXY formation.

3.4 Isothermal Calorimetry (IC)

Isothermal calorimetry was used to assess the heat release during the hydration of the cement pastes. The admixture was first dispersed in the batching water, and the cement was then loaded in the mixing bowl. The materials were mixed using a vacuum mixer for 90 s at 400 rpm and a 70% vacuum level. The mixing cup was scraped using a silicone spatula for 15s and vacuum mixing was carried out for an additional 90s. After mixing, around 7 g of the cementitious paste was transferred to a glass ampoule and sealed. The glass ampoules were then lowered into the isothermal calorimeter, which was pre-conditioned at 23 ± 0.05°C. Data was not collected for the first 45 minutes to allow for baseline stabilization. Heat flow and heat release were measured, and the data were collected for seven days. Two replicates were tested for each mixture.

3.5 Chloride profiling

ASTM 1556-22 [46] provides a standard test method for determining the chloride distribution in the sample after it is exposed to chloride ions at its surface, and the chloride ions diffuse into the sample. Specifically, 50.8 mm by 101.6 mm samples were cast and cured for 91 days in sealed conditions before being coated on the sides and bottom with an epoxy-based paint. The samples were then immersed in a 16.5% NaCl solution for 56 days. After immersion, the samples were taken out from the solution, washed with tap water quickly, and then dried for 1 day in a 50 ± 3% RH chamber at 23°C ± 1°C. After exposure, fifteen 1-mm layers were ground from the exposed surface. Chloride contents were first measured at 5-mm intervals (0–1, 4–5, 9–10, and 14–15 mm) to evaluate the depth of chloride penetration and identify potential differences between mixtures. This preliminary analysis showed no significant differences in chloride content between the investigated mixtures at any depth. Based on these results, additional intermediate layers were not

analyzed, as they were not expected to provide further insight into diffusion trends. The powders obtained were dissolved in a nitric acid solution, and then the total chloride content of each layer was determined by the automatic titration device [47].

3.6 Thermodynamic modelling

Thermodynamic modeling was performed to complement the experimental work and describe the role of admixtures on the composition of the hardened cementitious systems. The thermodynamic modeling was done using the GEMS3K software [48, 49] coupled with the default PSI/Nagra and CemData 18.01 database [50]. The model utilizes the chemical composition of the cementitious material (e.g., PLC), the chemical composition of SCM, SCM reactivity, and volumetric mixture proportions as inputs. The thermodynamic calculations [51-53] were coupled with kinetic models [54-56] to predict the volumes of the reaction products (e.g., CH content) as a function of DoH (i.e., time). In this study, the modified Parrot-Killoh (MPK) model [54, 57] was used to incorporate reaction kinetics by calculating the mass fraction of each binder component (clinker phases for the PLC and oxide phases for the SCM) that reacts at a given age. The maximum degree of reactivity (DOR*) of the SCMs used in the MPK model are obtained using PRT [35, 58, 59]. The approach has been validated extensively in previous studies [54, 55, 57, 60].

In this study, simulations were performed for quantifying the CH content as a function of DoH for (1) a control PLC mixture without any admixtures, (2) PLC mixtures containing Admixture A at two dosages of 32 and 64 oz/cwt (20.88 and 41.8 mL/kg), and (3) PLC mixtures with 5% silica fume. All mixtures had a w/b of 0.42. The admixture was assumed to be 100% SiO_2 with a DOR* of 58%, while silica fume was assumed to be 100% SiO_2 with a DOR* of 100%.

4 Results and discussion

4.1 Thermogravimetric analysis

The CH content of the samples, determined by TGA, is shown in Figure 3. The CH content of the reference system was 10.23 g/100 g of paste). The overall ability of a pozzolan to reduce CH depends on both the amount of material used and its pozzolanic reactivity. The CH values, for all the mixtures studied, remain within ± 20% of the reference mixture. This is expected given the relatively small amount of material introduced (0.08–1.35% of cement mass) into the paste as compared to more conventional SCMs. At low admixture dosages, CH content decreases (from 10.23 g in the plain cement system to 9.58 g and 8.90 g/100 g paste for A2 and B2, respectively). Interestingly, the CH increases again at higher dosages, reaching values comparable to or exceeding the control (11.78 g and 9.48 g/100 g paste for A5 and B5, respectively). This trend is counterintuitive, as higher dosages would generally be expected to increase CH consumption via the pozzolanic reaction.

The non-evaporable water content, shown on Figure 4, provides clarification on the higher CH content observed. Admixture A increases the non-evaporable water content with dosage, whereas admixture B shows no effect on the non-evaporable water content. The degree of hydration (DoH) is directly proportional to non-evaporable water content, and it implies that admixture A promotes higher DoH, which in turn leads to higher CH formation and offsets pozzolanic consumption. This increase in DoH is attributed to the additional nucleation sites provided by the NS. Based on the amount of silica introduced in the system, it is possible to calculate the CH that will be consumed by the pozzolanic reaction. Theoretically predicted CH consumptions have been computed and are shown on Figure 3. Theoretical CH consumption due to pozzolanic reaction was estimated from the nano-silica admixture solid content, its measured pozzolanic reactivity (PRT), and the reaction stoichiometry. The calculation assumes that the entire solid content of the admixture is silica and that the pozzolanic reaction produces Ca-poor C-S-H with a Ca/Si ratio of 1.6.

The black solid line represents the expected CH content assuming constant DoH, while the red dashed and blue dotted lines account for changes in DoH induced by admixtures A and B. Measured CH values at low dosages are consistently below the predicted values, suggesting either higher-than-expected pozzolanic reactivity or reduced hydration. Given the non-evaporable water data, reduced hydration can be excluded, supporting the hypothesis of increased pozzolanic reactivity at lower dosages which is possibly due to greater availability of unreacted CH. The PRT test conditions (Section 3.1) yield a much higher colloidal silica/CH ratio (0.11) than the mortar mixtures (0.005 for A1 to 0.08 for A5), equivalent to an admixture dosage of ~95 oz/cwt (~62 mL/kg). Thus, reactivity at lower dosages may have been underestimated, which could explain part of the discrepancy between measured and predicted CH values.

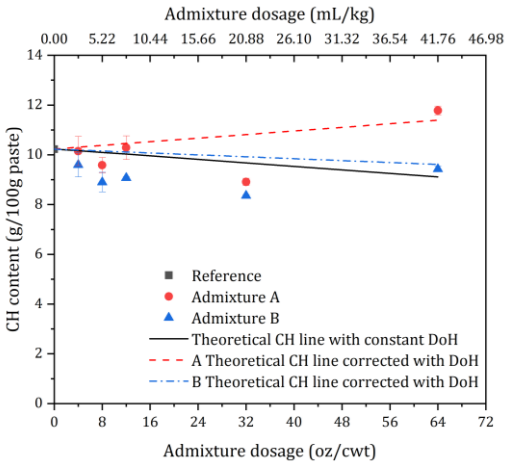

Figure 3. CH measurements for the mortar prepared with different admixture dosages. Theoretically predicted values are shown using dashed lines and correspond to the amount of CH consumed by the pozzolanic reaction due to the addition of the specified amount of NS.

Figure 5 relates the DoH to CH content. Experimental results are compared with thermodynamic model predictions for the control mixture and admixture dosages of 32 and 64 oz/cwt

(20.88 and 41.8 mL/kg). For reference, a curve for PLC with 5% silica fume is also shown, highlighting the small scale of the pozzolanic reaction observed in these systems. Thermodynamic calculations of the mixtures with admixtures confirm the experimental data. Thermodynamic calculations also show that even though the admixtures provide some reactive silica that act pozzolanically; this amount is rather small in the studied admixture dosages (i.e., 32 oz and 64 oz/cwt) (20.9 and 41.8 mL/kg), as indicated by the small decrease in the CH content. In comparison, thermodynamic calculations show that 5% reactive silica fume addition results in considerably pozzolanic reactions that reduce the CH content of the mixtures by about 35%.

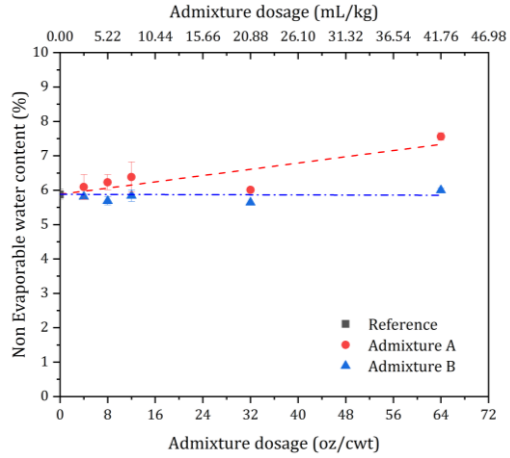

Figure 4. Non evaporable water content measurements on the mortar prepared with different admixture dosages.

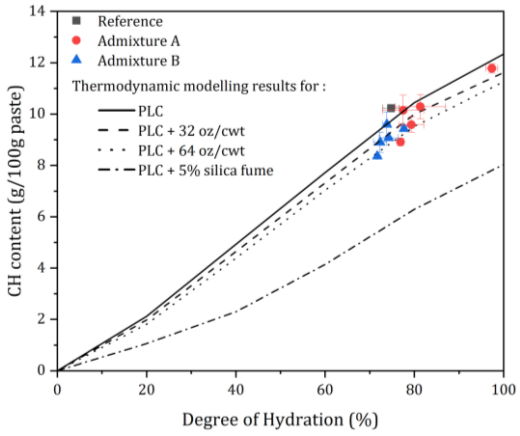

Figure 5. Relationship between the CH content and the degree of hydration of the studied mixtures. Modelling results presenting the expected value for PLC, PLC + 32 oz/cwt (20.88 mL/kg), PLC + 64 oz/cwt (41.8 mL/kg) and PLC + 5% (wt.) silica fume are also shown.

Figure 6 illustrates the CH consumed as a function of SCM dosage. The results of the admixtures are shown along with other SCMs like silica fume and fly ash [61, 62]. CH content for cement blends containing ground granulated blast furnace slags or calcined clays are also available in previous studies [63, 64]. Figure 6a shows the relatively low SCM addition rates of the admixtures as compared to the more conventional SCMs. Figure 6b zooms in on the lower admixture dosages and shows that up to an addition of 32 fl oz/cwt (20.9 mL/kg) the CH has a generally decreasing trend, however this increases for higher additions.

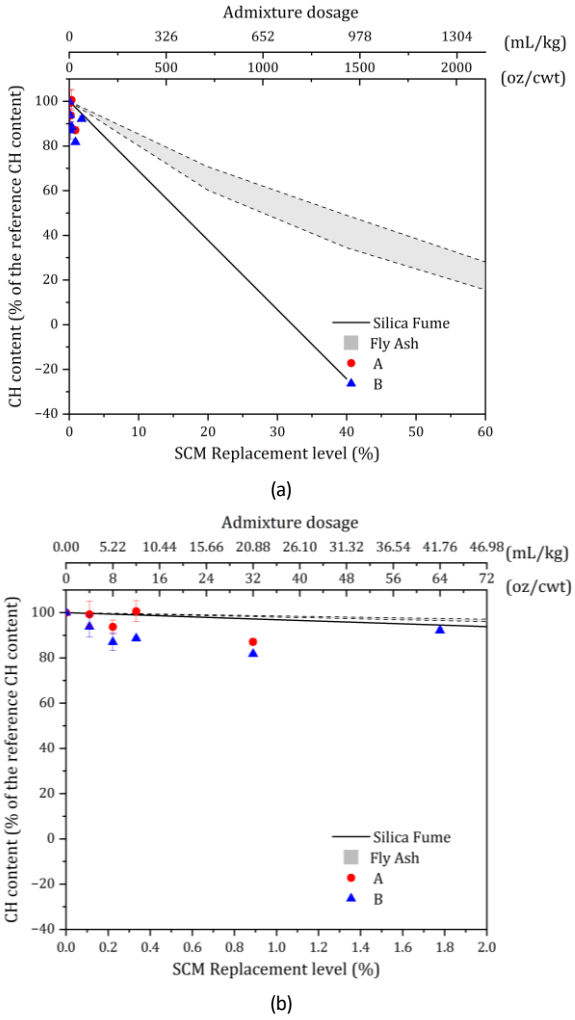

Figure 6. Comparison between the CH consumption of the studied admixtures and the corresponding silica fume replacement level (in vol%).

4.2 Low Temperature Differential Scanning Calorimetry (LT-DSC)

Figure 7 presents the measured CaOXY contents obtained from LT-DSC as a function of admixture dosage. The trends observed for CaOXY follow those of CH, and the same observations made in Figure 3 apply here. As admixture dosage increases, CaOXY values first decrease due to the pozzolanic reaction and CH consumption (CaOXY reducing from 32.7g in the plain cement system to 22.8 g and 23.6 g/100 g paste for A2 and B2, respectively), then rise again as a result of the higher degree of hydration (35.0 g and 40.5 g/100 g paste for A5 and B5, respectively), as discussed in Section 4.1. All these results are comprised within +20% and -30% of the reference value. Westbrook et al. [65] have shown similar results with CaOXY values close or slightly higher than the reference system. This has been attributed to increased

hydration due to a nucleation effect [66] and corroborates the previous hypothesis.

The relationship between CaOXY and CH content for all tested samples is also shown in Figure 8, along with a theoretical line derived from reaction stoichiometry (molar ratio of 2.47, corresponding to the molecular weight of CaOXY, 549, divided by three times that of CH, 74).

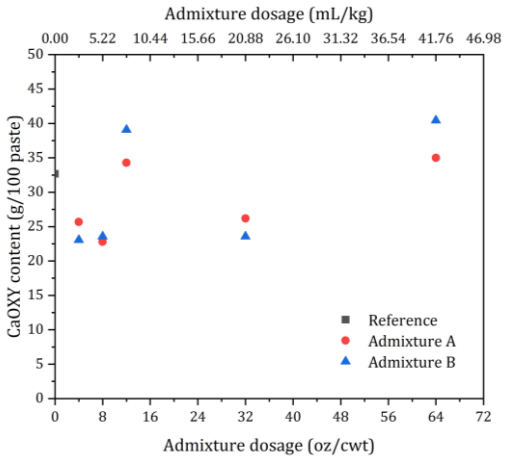

Figure 7. CAOXY measurements for the mortar prepared with different admixture dosages.

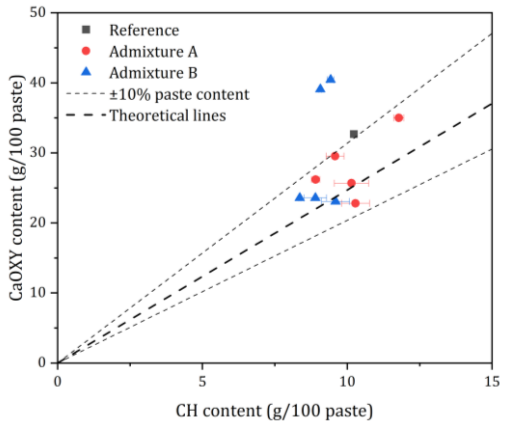

Figure 8. Relationship between the CH content and the CAOXY content for the mixtures studied. Theoretically predicted values of CAOXY are shown using a dashed line passing through origin and having slope of 2.47.

4.3 Isothermal Calorimetry

Figure 9 shows the cumulative heat release (J/g of binder) for pastes prepared with different admixture dosages. The cumulative heat release is largely unaffected by dosage, increasing only slightly from 304.2 to 314.2 J/g of binder for admixture A and 314.5 J/g of binder for admixture (a 3% increase) between 0 and 64 oz/cwt (41.76 mL/ kg).

The heat flow during the first 24 hours is shown in Figure 10. While admixture B led to a slight increase in the heat flux to 4.38 mW/g of binder from 4.22 mW/g of binder for the reference mixture, the curves show marginal differences in hydration rate or in the position of the tricalcium aluminate or calcium silicate peaks.

Overall, these results indicate that both admixture A and admixture B are responsible for a slight increase in hydration but that neither significantly influences hydration kinetics for the dosages considered.

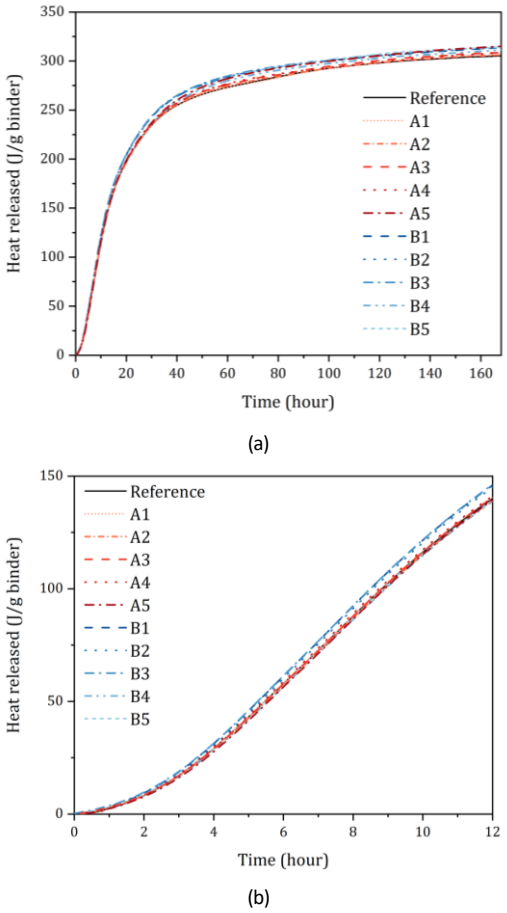

Figure 9. Total heat released per g of binder in paste with varying dosage of admixture over (a) 7 days and (b) the first 12 hours.

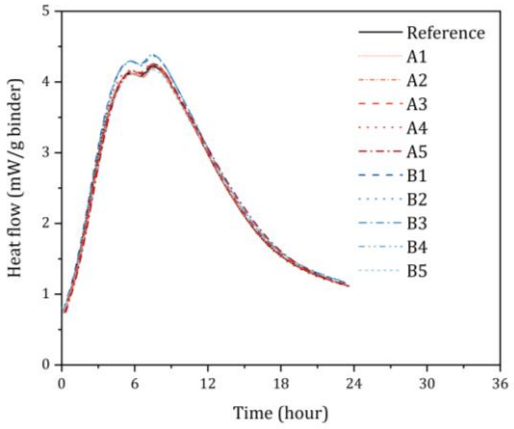

Figure 10. Early heat released per g of binder in paste with varying dosage of admixture.

4.4 Chloride Profile

The acid-soluble chloride profiles of samples immersed into 16.5% NaCl solution for 56 days were determined. The results show no significant difference between the control and the mixtures prepared with admixtures A or B. Across all tested layers, the measured chloride contents are comprised between ± 0.10% (of the sample mass) of the control values (control standard deviation: ± 0.05%).

In the surface layer (0–1 mm), chloride contents were 0.94%, 0.82%, and 0.95% for admixture A (4, 8, and 12 oz/cwt) (2.6, 5.2, 7.8 mL/kg), 0.88%, 0.89%, and 0.93% for admixture B, and 0.91% for the reference. At greater depth (9–10 mm), the corresponding values were 0.20%, 0.21%, and 0.14% for admixture A, 0.22%, 0.26%, and 0.16% for admixture B, and 0.23% for the reference.

Based on these measurements, the projected surface chloride concentration and the apparent chloride diffusion coefficient were computed using non-linear regression analysis as described in ASTM C1556 [46] and are presented in Table 3.

The diffusion coefficients obtained are all within ± 15% of the control, confirming that neither admixture A nor B has a significant effect on chloride ingress. The lack of significant effect of the nano-silica admixtures on chloride ingress may be explained by the very low dosage levels of the NS used which limit the amount of pozzolanic reaction, though the material is very reactive. At these dosages, the NS introduces only small amounts of reactive silica, resulting in minimal CH consumption and negligible refinement of the pore structure. Consequently, the transport properties controlling chloride diffusion remain largely unchanged. This observation is consistent with the earlier results, where the admixtures showed only limited pozzolanic behavior with minor influence on hydration, CH content and CaOXY formation.

Table 3. Project surface chloride concentration and apparent chloride diffusion coefficient computed using non-linear regression analysis.

	Ref	A1	A2	A3	B1	B2	B3
C_s (% of sample mass)	0.92	0.89	0.86	0.92	0.91	0.96	0.99
D_A (1.10^{-12} m^2/s)	3.98	4.44	3.27	3.67	4.51	3.82	3.45

5 Conclusions

This paper examines commercially available nano silica (NS) admixtures designed to improve placing and finishing concrete on-site. Specifically, this paper explores if the expected benefits from NS could be achieved at the dosages they are typically used in practice. The main objective of this paper is to provide answers to some of these questions by studying two NS admixtures (labeled A and B).

Some of the conclusions of the work include:

- Admixture A has a solid content of 31.8%, and admixture B has a solid content of 32.4%. These solid contents correspond to silica contents in the samples of 0.08 % and 1.35% of cement mass respectively. These are rather low silica contents as compared to more conventional SCMs like silica fume or fly ash.
- Pozzolanic Reactivity Testing (PRT) showed that NS had a reactivity of 58% for Admixture A and 41% for Admixture B. These reactivities are higher than those of a large range of siliceous pozzolanic materials (e.g., fly ash); therefore, NS shows that it reacts pozzolanically. These reactivity levels are greater than many fly ashes and slightly less than silica fumes. Isothermal Calorimetry (IC) testing showed that the heat of hydration increased slightly when the NS was used (by 2% for admixture A and 3% for admixture B) as compared to the reference.
- Thermogravimetric Analysis (TGA) showed a 7% reduction in CH for admixture A and a 13% reduction in CH for admixture B at their typical dosage levels.
- At dosages higher than those used in practice there was an increase in the CH for admixture A. This was consistent with the 23% increase in degree of hydration that was observed based on non-evaporable water. Admixture B, on the other hand, showed CH content consistent with the predicted CH consumption from the pozzolanic reaction corresponding to the amount of reactive silica introduced in the system.
- Low Temperature Differential Scanning Calorimetry (LTDSC) results indicated a reduction in calcium oxychloride potential for formation (30% for admixture A and 29% for material B) at low admixture dosages, which are slightly greater than the reduction in CH content. This effect is likely the result of coating the CH with a reactive product that makes the CH in the core less available to CAOXY formation. This reduction in CAOXY formation, however, is less than what is needed in many practical applications to control this reaction if no other SCM is used.
- Chloride ingress was measured on hardened mortars with neither admixture A nor B having a significant effect on the surface chloride concentration or the diffusion coefficient.
- Thermodynamic calculations of the mixtures with admixtures confirm the experimentally obtained CH contents with and without admixtures. Thermodynamic calculations show that even though the admixtures provide some reactive silica that act pozzolanically, this amount is rather small in the studied admixture dosages (i.e., 32 oz and 64 oz/cwt)(20.9 and 41.8 mL/kg), as indicated by the small decrease in the CH content. In comparison, thermodynamic calculations show that 5% reactive silica fume addition results in considerable pozzolanic reactions that reduce the CH content of the mixtures by about 35%.

Overall, while the nano-silica admixtures show measurable pozzolanic activity and minor reductions in CH and CaOXY

formation, the effects at practical dosage levels are limited. Consequently, these admixtures alone are unlikely to significantly enhance durability in typical field applications, and their use should be considered complementary to other SCMs or durability-enhancing strategies.

Authorship statement (CRediT)

Julien Hubert: Investigation; Writing – Original Draft; Writing – Review & Editing; Visualization; Project administration; Conceptualization. **Fengyin Du:** Investigation; Writing – Review & Editing; Visualistion; Data Curation. **Cibele De Araujo:** Investigation. **O Burkan Isgor:** Methodology; Writing – Review & Editing; Supervision; Project Administration; Funding Acquisition; Conceptualization; **W Jason Weiss:** Methodology; Writing – Original Draft; Supervision; Project Administration; Funding Acquisition; Conceptualization.

Acknowledgement

The authors would like to acknowledge Premiere Concrete Admixtures for their financial contribution that supports a part of this work.

Data availability

Data will be made available on reasonable request.

Declarations

The authors declare that they have no known competing financial interests or personal relationships that could have appeared to influence the work reported in this paper.

References

[1] P. Aggarwal, R. P. Singh, Y. Aggarwal, Use of nano-silica in cement based materials—A review, Cogent Eng (2015) 2 (1): 1078018. https://doi.org/10.1080/23311916.2015.1078018

[2] P. P. Abhilash, D. K. Nayak, B. Sangoju, R. Kumar, V. Kumar, Effect of nano-silica in concrete: A review, Constr Build Mater (2021) 278: 122347. https://doi.org/10.1016/j.conbuildmat.2021.122347

[3] J. S. Belkowitz, W. Belkowitz, K. Nawrocki, F. T. Fisher, Impact of nanosilica size and surface area on concrete properties, ACI Mater J (2015) 112 (3): 419–427. https://doi.org/10.14359/51687397

[4] J. S. Belkowitz, W. B. Belkowitz, R. D. Moser, F. T. Fisher, C. A. Weiss Jr., The influence of nano silica size and surface area on phase development, chemical shrinkage and compressive strength of cement composites, in: Nanotechnology in Construction (2015): 207–212. https://doi.org/10.1007/978-3-319-17088-6_26.

[5] P. Mondal, S. P. Shah, L. D. Marks, J. J. Gaitero, Comparative study of the effects of microsilica and nanosilica in concrete, Transp Res Rec (2010) 2141 (1): 6–9. https://doi.org/10.3141/2141-02

[6] P. K. Hou, S. Kawashima, K. J. Wang, D. J. Corr, J. S. Qian, S. P. Shah, Effects of colloidal nanosilica on rheological and mechanical properties of fly ash-cement mortar, Cem Concr Compos (2013) 35 (1): 12–22. https://doi.org/10.1016/j.cemconcomp.2012.08.027

[7] Y. Qing, Z. Zenan, S. Li, C. Rongshen, A comparative study on the pozzolanic activity between nano-SiO_2 and silica fume, J Wuhan Univ Technol Mater Sci Ed (2006) 21 (3): 153–157. https://doi.org/10.1007/BF02840907

[8] M. Collepardi, Self-compacting concrete: What is new?, in: Proc Seventh CANMET/ACI Int Conf on Superplasticizers and Other Chemical Admixtures in Concrete (2003).

[9] I. A. Sharaky, F. A. Megahed, M. H. Seleem, A. M. Badawy, The influence of silica fume, nano silica and mixing method on the strength and durability of concrete, SN Appl Sci (2019) 1 (6). https://doi.org/10.1007/s42452-019-0621-2

[10] L. Singh, S. Karade, S. Bhattacharyya, M. M. Yousuf, S. Ahalawat, Beneficial role of nanosilica in cement based materials—A review, Constr Build Mater (2013) 47: 1069–1077. https://doi.org/10.1016/j.conbuildmat.2013.05.052

[11] P. Hou, S. Kawashima, D. Kong, D. J. Corr, J. Qian, S. P. Shah, Modification effects of colloidal nanoSiO_2 on cement hydration and its gel property, Compos Part B Eng (2013) 45 (1): 440–448. https://doi.org/10.1016/j.compositesb.2012.05.056

[12] J. S. Belkowitz, An investigation of nano silica in the cement hydration process, University of Denver (2009).

[13] E. M. Gartner, F. J. Tang, S. J. Weiss, Saturation factors for calcium hydroxide and calcium sulfates in fresh Portland cement pastes, J Am Ceram Soc (1985) 68 (12): 667–673. https://doi.org/10.1111/j.1151-2916.1985.tb10122.x

[14] W. Fajun, M. W. Grutzeck, D. M. Roy, The retarding effects of fly ash upon the hydration of cement pastes: The first 24 hours, Cem Concr Res (1985) 15 (1): 174–184. https://doi.org/10.1016/0008-8846(85)90024-9

[15] J. Beaudoin, I. Odler, Hydration, setting and hardening, in: Lea's Chemistry of Cement and Concrete (2019): 157. https://doi.org/10.1016/B978-0-08-100773-0.00005-8

[16] G. Sant, B. Lothenbach, P. Juilland, G. Le Saout, J. Weiss, K. Scrivener, The origin of early age expansions induced in cementitious materials containing shrinkage reducing admixtures, Cem Concr Res (2011) 41 (3): 218–229. https://doi.org/10.1016/j.cemconres.2010.12.004

[17] H. Cheng-Yi, R. F. Feldman, Hydration reactions in Portland cement-silica fume blends, Cem Concr Res (1985) 15 (4): 585–592. https://doi.org/10.1016/0008-8846(85)90056-0

[18] A. Barberena-Fernández, P. Carmona-Quiroga, M. T. Blanco-Varela, Interaction of TEOS with cementitious materials: Chemical and physical effects, Cem Concr Compos (2015) 55: 145–152. https://doi.org/10.1016/j.cemconcomp.2014.09.010

[19] E. Franzoni, B. Pigino, A. Leemann, P. Lura, Use of TEOS for fired-clay bricks consolidation, Mater Struct (2014) 47 (7): 1175–1184. https://doi.org/10.1617/s11527-013-0120-7

[20] F. Sandrolini, E. Franzoni, B. Pigino, Ethyl silicate for surface treatment of concrete—Part I: Pozzolanic effect of ethyl silicate, Cem Concr Compos (2012) 34 (3): 306–312. https://doi.org/10.1016/j.cemconcomp.2011.12.003

[21] J. J. Gaitero Redondo, Multi-scale study of the fibre-matrix interface and calcium leaching in high performance concretes, Universidad del País Vasco (2008).

[22] J. Yang, W. Zuo, Z. Wu, W. She, Towards a deeper understanding of the impact of tetraethoxysilane (TEOS) on early-age cement hydration, Constr Build Mater (2024) 450: 138624. https://doi.org/10.1016/j.conbuildmat.2024.138624

[23] M. D. Niemuth, Effect of fly ash on the optimum sulfate of Portland cement, Purdue University (2012).

[24] E5 Liquid Fly Ash. Available: https://www.e5nanosilica.com/#:~:text=After%20rigorous%20testing%20and%20project,seen%20with%20any%20other%20admixtures

[25] Indiana Department of Transportation, Construction Memorandum 25-02: E5 Internal Cure and E5 Liquid Fly Ash in Concrete (2025).

[26] C. Huang, T. Nantung, Y. Feng, N. Lu, Effect of colloidal nano silica on the freeze-thaw resistance and air void system of Portland cement concrete, J Build Eng (2024) 86: 108888. https://doi.org/10.1016/j.jobe.2024.108888

[27] J. Watt, Concrete innovations coming soon to a pavement near you (2021).

[28] ASTM, ASTM C595-08a – Standard specification for blended hydraulic cements (2010).

[29] ASTM, ASTM C778-21 – Standard specification for standard sand (2021).

[30] ASTM, ASTM C494/C494M-24 – Standard specification for chemical admixtures for concrete (2024).

[31] Premiere Concrete Admixtures, UltraFinish 1L – Integral concrete finishing aid and viscosity modifying admixture specifically designed for Type 1L cement, Product Data Sheet (2025).

[32] E5 Liquid Fly Ash, Technical Data Sheet (2025).

[33] D. Glosser, A. Choudhary, O. B. Isgor, W. J. Weiss, Investigation of reactivity of fly ash and its effect on mixture properties, ACI Mater J (2019) 116 (4): 193–200. https://doi.org/10.14359/51716722
[34] D. Glosser, P. Suraneni, O. B. Isgor, W. J. Weiss, Using glass content to determine the reactivity of fly ash for thermodynamic calculations, Cem Concr Compos (2021) 115: 103849. https://doi.org/10.1016/j.cemconcomp.2020.103849
[35] P. Suraneni, J. Weiss, Examining the pozzolanicity of supplementary cementitious materials using isothermal calorimetry and thermogravimetric analysis, Cem Concr Compos (2017) 83: 273–278. https://doi.org/10.1016/j.cemconcomp.2017.07.009
[36] A. T. Coyle, R. P. Spragg, P. Suraneni, A. N. Amirkhanian, M. Tsui-Chang, W. J. Weiss, Activation energy of conduction for use in temperature corrections on electrical measurements of concrete, Adv Civ Eng Mater (2019) 8 (1): 158–170. https://doi.org/10.1520/ACEM20180045
[37] P. Suraneni, A. Hajibabaee, S. Ramanathan, Y. Wang, J. Weiss, New insights from reactivity testing of supplementary cementitious materials, Cem Concr Compos (2019) 103: 331–338. https://doi.org/10.1016/j.cemconcomp.2019.05.017
[38] K. Bharadwaj, O. B. Isgor, W. J. Weiss, A simplified approach to determine pozzolanic reactivity of commercial supplementary cementitious materials, Toward Development of Performance-Based Concrete Mixtures Made with Modern Cementitious Materials Using Thermodynamic Modelling (2022) 20.
[39] K. Bharadwaj, O. B. Isgor, W. J. Weiss, A literature-based dataset containing statistical compositions and reactivities of commercial and novel supplementary cementitious materials, Oregon State University (2022).
[40] Premiere Concrete Admixtures, Safety data sheet: UltraFinish 1L (2025).
[41] E5 Liquid Fly Ash, Safety data sheet (2025).
[42] T. Kim, J. Olek, Effects of sample preparation and interpretation of thermogravimetric curves on calcium hydroxide in hydrated pastes and mortars, Transp Res Rec (2012) 2290 (1): 10–18. https://doi.org/10.3141/2290-02
[43] AASHTO T 365-20 – Standard method of test for quantifying calcium oxychloride formation potential of cementitious pastes exposed to deicing salts (2020).
[44] J. Monical, E. Unal, T. Barrett, Y. Farnam, W. J. Weiss, Reducing joint damage in concrete pavements: Quantifying calcium oxychloride formation, Transp Res Rec (2016) 2577 (1): 17–24. https://doi.org/10.3141/2577-03
[45] Y. Farnam, S. Dick, A. Wiese, J. Davis, D. P. Bentz, J. Weiss, The influence of calcium chloride deicing salt on phase changes and damage development in cementitious materials, Cem Concr Compos (2015) 64: 1–15. https://doi.org/10.1016/j.cemconcomp.2015.09.006
[46] ASTM, ASTM C1556-22 – Standard test method for determining the apparent chloride diffusion coefficient of cementitious mixtures by bulk diffusion (2022).
[47] C. Di Bella, C. Villani, E. Hausheer, J. Weiss, Chloride transport measurements for a plain and internally cured concrete mixture, ACI Spec Publ (2012) 290: 1–16.
[48] D. A. Kulik, Improving the structural consistency of C–S–H solid solution thermodynamic models, Cem Concr Res (2011) 41 (5): 477–495. https://doi.org/10.1016/j.cemconres.2011.01.012
[49] D. A. Kulik, T. Wagner, S. V. Dmytrieva, G. Kosakowski, F. F. Hingerl, K. V. Chudnenko, U. R. Berner, GEM-Selektor geochemical modeling package: Revised algorithm and GEMS3K numerical kernel for coupled simulation codes, Comput Geosci (2013) 17 (1): 1–24. https://doi.org/10.1007/s10596-012-9310-6
[50] B. Lothenbach, D. A. Kulik, T. Matschei, M. Balonis, L. Baquerizo, B. Dilnesa, G. D. Miron, R. J. Myers, Cemdata18: A chemical thermodynamic database for hydrated Portland cements and alkali-activated materials, Cem Concr Res (2019) 115: 472–506. https://doi.org/10.1016/j.cemconres.2018.04.018
[51] B. Lothenbach, T. Matschei, G. Möschner, F. P. Glasser, Thermodynamic modelling of the effect of temperature on the hydration and porosity of Portland cement, Cem Concr Res (2008) 38 (1): 1–18. https://doi.org/10.1016/j.cemconres.2007.08.017
[52] B. Lothenbach, F. Winnefeld, Thermodynamic modelling of the hydration of Portland cement, Cem Concr Res (2006) 36 (2): 209–226. https://doi.org/10.1016/j.cemconres.2005.03.001
[53] B. Lothenbach, M. Zajac, Application of thermodynamic modelling to hydrated cements, Cem Concr Res (2019) 123: 105779. https://doi.org/10.1016/j.cemconres.2019.105779
[54] D. Glosser, O. B. Isgor, W. J. Weiss, Non-equilibrium thermodynamic modeling framework for ordinary Portland cement/supplementary cementitious material systems, ACI Mater J (2021) 117 (6). https://doi.org/10.14359/51728127
[55] D. Glosser, P. Suraneni, O. B. Isgor, W. J. Weiss, Estimating reaction kinetics of cementitious pastes containing fly ash, Cem Concr Compos (2020) 112: 103655. https://doi.org/10.1016/j.cemconcomp.2020.103655
[56] L. J. Parrot, D. Killoh, Prediction of cement hydration, in: Proc Br Ceram Soc (1984) 35: 41–53.
[57] D. B. Glosser, Equilibrium and non-equilibrium thermodynamic modeling of cement pastes containing supplementary cementitious materials (2020).
[58] K. Bharadwaj, O. B. Isgor, J. W. Weiss, A simplified approach to determine the pozzolanic reactivity of commercial supplementary cementitious materials, Concr Int (2022) 44 (1): 27–32. https://doi.org/10.14359/51734415
[59] A. Choudhary, K. Bharadwaj, R. M. Ghantous, O. B. Isgor, J. Weiss, Pozzolanic reactivity test of supplementary cementitious materials, ACI Mater J (2022) 119 (2): 255–268. https://doi.org/10.14359/51734349
[60] K. Bharadwaj, D. Glosser, M. K. Moradllo, O. B. Isgor, W. J. Weiss, Toward the prediction of pore volumes and freeze-thaw performance of concrete using thermodynamic modelling, Cem Concr Res (2019) 124: 105820. https://doi.org/10.1016/j.cemconres.2019.105820
[61] S. N. Whatley, P. Suraneni, V. J. Azad, O. B. Isgor, J. Weiss, Mitigation of calcium oxychloride formation in cement pastes using undensified silica fume, J Mater Civ Eng (2017) 29 (10): 04017198. https://doi.org/10.1061/(ASCE)MT.1943-5533.0002052
[62] P. Suraneni, V. J. Azad, O. B. Isgor, W. J. Weiss, Use of fly ash to minimize deicing salt damage in concrete pavements, Transp Res Rec (2017) 2629 (1): 24–32. https://doi.org/10.3141/2629-05
[63] P. Suraneni, V. J. Azad, O. B. Isgor, W. J. Weiss, Calcium oxychloride formation in pastes containing supplementary cementitious materials: Thoughts on the role of cement and supplementary cementitious materials reactivity, RILEM Tech Lett (2016) 1: 24–30. https://doi.org/10.21809/rilemtechlett.2016.7
[64] P. Suraneni, V. J. Azad, O. B. Isgor, J. Weiss, Role of supplementary cementitious material type in the mitigation of calcium oxychloride formation in cementitious pastes, J Mater Civ Eng (2018) 30 (10): 04018248. https://doi.org/10.1061/(ASCE)MT.1943-5533.0002425
[65] M. A. Westbrook, R. M. Ghantous, W. J. Weiss, J. S. Belkowitz, Utilizing nano silica to reduce calcium oxychloride formation in cementitious materials, Transp Res Rec (2023) 2677 (3): 1542–1550. https://doi.org/10.1177/03611981221125209
[66] G. Land, D. Stephan, The influence of nano-silica on the hydration of ordinary Portland cement, J Mater Sci (2012) 47 (2): 1011–1017 https://doi.org/10.1007/s10853-011-5881-1